Heliyon 9 (2023) e20124

Contents lists available at ScienceDirect

Heliyon

journal homepage: www.cell.com/heliyon

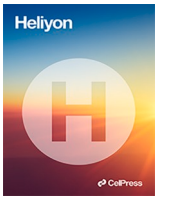

IL-1β-pretreated bone mesenchymal stem cell-derived exosomes alleviate septic endoplasmic reticulum stress via regulating SIRT1/ERK pathway

Xinsheng Cheng [a,b,1], Shikai Wang [b,1], Zhipeng Li [b], Di He [b], Jianguo Wu [b], Weiwei Ding [a,*]

[a] Division of Trauma and Acute Care Surgery, Department of Surgery, Jinling Hospital, Affiliated Hospital of Medical School, Nanjing University, Nanjing, Jiangsu Province, China
[b] Department of Hepatobiliary and Pancreatic Surgery, Union Shenzhen Hospital, Huazhong University of Science and Technology, Shenzhen, Guangdong, China

ARTICLE INFO

Keywords:
Sepsis
Mesenchymal stem cells
Exosomes
SIRT1
ER stress

ABSTRACT

Background: Endoplasmic reticulum (ER) plays a crucial role in the development of organ injury caused by sepsis. Therefore, it is highly important to devise strategies that specially target ER stress for the treatment of sepsis. Previous research has shown that priming chemokines can enhance the therapeutic effects of mesenchymal stem cells (MSCs). In this study, we aimed to investigate the function and mechanism of exosomes derived from MSCs that were pretreated with IL-1β (IB-exos) in the context of septic ER stress.

Methods: Mouse bone MSCs were preconditioned with or without IL-1β and the supernatant was used for exosome extraction. In vitro sepsis cell mode was induced by treating HUVECs with LPS, while in vivo sepsis model was established through cecal ligation and puncture (CLP) operation in mice. Cell viability, apoptosis, motility, and tube formation were assessed using the EDU proliferation assay, flow cytometry analysis, migration assay, and tube formation assay, respectively. The molecular mechanism was investigated using ELISA, qRT-PCR, Western blot, and immunofluorescence staining.

Results: Pretreatment with IL-1β enhanced the positive impact of MSC-exos on the viability, apoptosis, motility, and tube formation ability of HUVECs. The administration of LPS or CLP increased ER stress response, but this effect was blocked by the treatment of IB-exos. Additionally, IB-exos reversed the inhibitory effects of LPS or CLP on the expression levels of SIRT1 and ERK phosphorylation. Knockdown of SIRT1 counteracted the effects of IB-exos on HUVEC cellular function and ER stress. In a mouse model, the injection of IB-exos mitigated sepsis-induced lung injury by inhibiting ER stress response through the activation of SIRT1.

Conclusion: IB-exos have been found to alleviate sepsis-induced lung injury via inhibiting ER stress through the SIRT1/ERK pathway. These findings indicated that IB-exos could potentially be used as a strategy to mitigate lung injury caused by sepsis.

* Corresponding author. Division of Trauma and Acute Care Surgery, Department of Surgery, Jinling Hospital, Affiliated Hospital of Medical School, Nanjing University, Nanjing, Jiangsu Province, China.
E-mail address: 83551571@qq.com (W. Ding).
[1] These authors were considered as the first authors since they contributed equally to this work.

https://doi.org/10.1016/j.heliyon.2023.e20124
Received 21 June 2023; Received in revised form 10 September 2023; Accepted 12 September 2023
Available online 13 September 2023

1. Introduction

Sepsis is an overwhelming response to infection which leads to significant morbidity and mortality [1]. Despite advancements in antibiotic therapy, cardiorespiratory resuscitation, glucose control, and ventilator management, there is currently no satisfactory treatments for sepsis [2]. Hence, is still necessary to develop effective strategies to address sepsis. Targeting the critical events or molecules involved in the progression of sepsis could offer new approaches for its treatment.

Multiple mechanisms, including immune regulation, inflammation response, macrophage polarization, and endothelial cell dysfunction, have be reported to contribute to the progression of sepsis [3,4]. Recent studies also suggest that endoplasmic reticulum (ER) stress plays a significant role in sepsis [5]. The ER, a critical intracellular organelle responsible for protein folding, post-translational modification, and secretion [6], can experience stress when there is an accumulation of unfolded or misfolded proteins [7]. It is known that ER stress can trigger inflammation and ER dysfunction, both of which play important roles in sepsis [8,9]. Therefore, targeting ER stress is considered an attractive strategy against sepsis [5].

Mesenchymal stem cells (MSCs) are a type of stromal cell that possess self-renew capability and multilineage differentiation potential [10]. MSCs exhibit a variety of bioactivities, such as immune modulation, anti-inflammation, anti-apoptosis, anti-ferroptosis, and pro-angiogenesis [11]. Extensive research has been conducted into the therapeutic potential of MSCs in a range of diseases, including sepsis [12–14]. MSCs have been shown to reduce bacterial load and inflammatory chemokine levels, thereby alleviating sepsis [15] and decrease mortality rates in septic rodents [16]. Additionally, a clinical study has indicated that the infusion of adipose-derived MSCs improves the survival rates of sepsis patients [17].

It is currently recognized that MSCs exert their effects through secreting exosomes [18], which are extracellular vesicles. Exosomes are responsible for transporting various biomolecules, including proteins, lipids, and nucleic acids to target cells [19]. Notably, exosomes have significant roles in crucial biological processes, such as cell survival, apoptosis, and cell migration [18–21]. Studies have revealed that exosomes carry increased levels of damage-associated molecular patterns (DAMPs) and cytokines, which trigger an inflammatory response in sepsis [22]. The administration of exosomes derived from human umbilical cord MSCs has been demonstrated to alleviate sepsis-induced acute kidney injury and improve the survival rate of mice with sepsis [23]. Similarly, exosomes from human placenta choriodecidual membrane-derived MSCs have been observed to mitigate lung injury induced by sepsis [20]. These findings suggest that hold promising therapeutic potential in the treatment of sepsis.

Previous studies have indicated that pretreatment with inflammatory cytokines can augment the immunoregulatory capabilities of MSCs and subsequently increase their therapeutic effectiveness [24,25]. The present study aimed to examine whether exosomes produced by IL-1β primed MSCs exhibit heightened efficacy in treating sepsis and evaluate the potential mechanisms linked to ER stress.

2. Materials and methods

2.1. Cell culture and reagents

Human umbilical vein vascular endothelial cells (HUVECs) and C57Bl/6J mouse bone mesenchymal stem cells (BMSCs) were obtained from Guangzhou Cyagen Company (Guangzhou, China). EGM-2 MV Medium (Lonza, Switzerland) containing 10% FBS and 1% penicillin-streptomycin was used for the culture of HUVECs. The medium for human mesenchymal stem cells (Cyagen Biosciences) was applied for the culture of mouse BMSCs. BMSCs at passage 3–5 was used in this study. LPS and IL-1β was purchased from Sigma (USA) and R&D systems (USA), respectively. For inducing the in vitro sepsis model, HUVECs were cultured in medium containing 10 μg/ml LPS for 24 h.

2.2. Isolation of exosomes from mouse BMSCs

Mouse BMSCs were cultured in medium alone or containing 10 ng/ml IL-1β for 12 h. The supernatant was harvested and used for the purification of exosomes. To isolate exosomes, BMSCs were pelleted by centrifugation at 3000 rpm for 15 min at 4 °C. To remove cell debris, the supernatant was centrifuged at 20,000 g for 45 min at 4 °C. Then the supernatant was transferred to a new tube and centrifuged at 110,000 g for 70 min at 4 °C. After washing with PBS once, the pellet was centrifuged again at 110,000 g for 70 min at 4 °C. The pellet was collected, resuspended in PBS, filtrated with a 0.22 μm membrane, and kept at −80 °C.

2.3. Transmission electron microscopy

For detecting the morphology of ER, lung tissues were fixed in 2.5% glutaraldehyde for 2 h and 1% OsO4 for 2 h. The lung tissues were embedded in resin. Ultrathin sections were cut and stained with uranyl acetate and lead citrate. The sections were visualized using a transmission electron microscope (JEOL, Japan). For detecting the morphology of exosomes, an aliquot of exosome suspension was placed on a carbon-coated copper grid. After air dried for 30 min at room temperature, the grid was kept in glutaraldehyde (3%) for 15 min. The grid was then placed in 2% uranyl acetate solution for 5 min for staining. The grid was observed under a transmission electron microscope (JEOL, Japan). The exosome size was analyzed by nanoparticle tracking analysis (NTA).

2.4. The uptake of exosomes by HUVECs

Exosomes were labeled using PKH67 dye (Sigma, USA). HUVECs were cultured overnight in 6-well plates. 2 μg PKH67-labeled exosomes were added to the culture medium and incubation was performed for 24 h. HUVECs were fixed with 4% paraformaldehyde and nuclei were stained with DAPI. Observation of HUVECs was conducted using a confocal microscopy (Carl Zeiss, Germany).

2.5. EDU proliferation assay

HUVECs (3.5×10^4 cells/well) were seeded in 24-well plates and cultured overnight. The medium was removed and cells were washed once with PBS. Then serum-free medium containing 10 μmol/L EDU (5-ethynyl-2′-deoxyuridine) (RiboBio, Guangzhou, China) was added to the plate and incubation was lasted for 2 h. After fixation with 4% paraformaldehyde, cells were stained with Apollo dye solution for proliferating cells. Nuclei were stained with DAPI. Proliferating cells were observed using a fluorescence microscopy.

2.6. Transwell migration assay

The motility of HUVECs was addressed using the tanswell migration assay. Transwells were purchased from Corning company (USA). Cells (2.5×10^4) were plated into the upper chamber (Corning, USA) in a serum-free medium, while the lower chamber containing 600 μl completed medium with 10 μg/ml exosomes. After incubation at 37 °C for 24 h, cells were fixed with pre-cooled methanol. After staining with 0.05% crystal violet, the number of cells that was migrated to the bottom side of the membrane was counted.

2.7. Tube formation assay

The 24-well plate was precoated with Matrigel (BD Sciences, USA) before cell seeding. HUVECs was serum-starved with medium with 0.2% FBS for 6 h. 2.5×10^4 HUVECs were seeded in the pre-coated 24-well plate. Medium containing 10 μg/ml exosomes were added to each well. After incubation for 24 h, the formation of HUVEC cell tubes was examined and the number of tubes was counted under a light microscope.

2.8. Quantitative RT-PCR assay

HUVECs were cultured in 6-well plated in medium alone or containing exosomes (10 μg/ml). After cultured for 24 h, HUVECs were harvested and used for RNA isolation. Trizol reagent (Life Science, USA) was used for RNA isolation. First-strand cDNA was synthesized using random hexamer primers and a M-MLV reverse transcriptase kit (Promega). PCR amplification was performed using the SYBR Green I PCR kit (QIAGEN) on an Applied Biosystems 7300 system (Applied Biosystems, USA). The $2^{-\Delta\Delta CT}$ formula was used for relative quantification of gene expression. The data was normalized to GAPDH.

2.9. siRNA transfection

Control siRNA and siRNA targeting SIRT1 were purchased from GenePharm (Shanghai, China). siRNA transfection was conducted using Lipofectamine 2000 reagent (ThermoFisher, USA) according to the manufacturer's introductions.

2.10. ELISA assay

The serum concentration of IL-1β, IL-6, and TNF-a were determined using a mouse TNF-α ELISA kit (ab208348, Abcam), a mouse IL-6 ELISA kit (ab100712, Abcam), and a mouse IL-1β ELISA kit (ab100704, Abcam) according to the manufacture's introductions, respectively.

2.11. Western blot analysis

HUVECs or exosomes were collected and lysed using RIPA lysis buffer. Protein concentration was determined using the BCA method. 30 μg proteins were subjected to SDS-PAGE gel and transferred onto the PVDF membrane (Millipore, USA). After blocking in 5% non-fat milk diluted in TBS-Tween 20 (TBST) for 60 min at room temperature, the membrane was incubated with specific antibody overnight at 4 °C. After three washes with TBST, the membrane was probed with secondary antibody. Protein signal was detected using a chemiluminescence detection kit (Beyotime Institute of Biotechnology, Shanghai, China).

2.12. Apoptosis analysis

The apoptosis rate was determined by flow cytometry using an Annexin V-FITC apoptosis detection kit (BD, USA). 3.5×10^5 HUVECs were plated in 6-well plates and treated with or without 10 μg/ml LPS in the presence or absence of 10 μg/ml exosomes. Following 24 h of incubation, HUVECs were harvested, centrifugated, and rinsed with PBS. HUVECs were resuspended with binding

buffer and incubated with 5 μl FITC-labeled Annexin V and 5 μl PI for 15 min at room temperature. The Samples were examined using a FACScan flow cytometer (BD Biosciences).

2.13. Animal experiments

Mouse sepsis model was established by the cecal ligation and puncture (CLP) operation as described previously [26]. BALB/c mice (21∼25g, male or female) from Guangdong Experimental Animal Center (Guangzhou, China) were fed adaptively for 1 week and fasted for 12 h before the experiment. After being anesthetized by intraperitoneal injection of pentobarbital sodium at a dose of 50 mg/kg body weight, mice were supine fixed on an operating plate. The hair of abdominal operational area was removed and the abdominal operational area was disinfected. Under sterile conditions, a 2 cm incision was made in the abdominal wall. Then the cecum was exteriorized and ligated distal to the ileocecal valve with 3–0 silk thread. The ligation part was punctured twice with an 18-gauge needle. Then the peritoneum and the skin were sutured discontinuously with 4–0 silk thread. At the same time, normal saline 50 ml/kg body weight was injected subcutaneously to prevent shock. In the control mice, the cecum was exteriorized without ligation or puncture. At 4 h after CLP operation, B-exos, IB-exos (2 μg/kg body weight) or PBS were intravenously injected into mice. At 24 h post-injection, mice were anesthetized by intraperitoneal injection of pentobarbital sodium (50 mg/kg body weight) and sacrificed by cervical dislocation. Then, the lung tissues were dissected for further experiments. Animal experiments were conducted under the approval of the Institutional Animal Care and Use Committee of Union Shenzhen Hospital of Huazhong University of Science and Technology (SYT23006).

2.14. Immunofluorescence staining

Frozen lung tissues or HUVECs cultured in coverslips were fixed in 4% paraformaldehyde. The tissues and HUVCEs were permeabilized with 0.1% Triton X-100 in PBS for 30 min at room temperature. Following washing with PBS, tissues or HUVECs were blocked with 5% BSA in PBS. The tissues or HUVECs were immersed with specific antibodies at 4 °C overnight. Following washing with PBS, tissues and HUVECs were immersed with an anti-mouse antibody conjugated to Alexa Fluor 488 or an anti-rabbit antibody conjugated to Alexa Fluor 594 (1:500 dilution, Life Technologies, USA) for 1 h at room temperature. Nuclei were stained with DAPI. The image was examined under a fluorescence microscope (Zeiss, Germany).

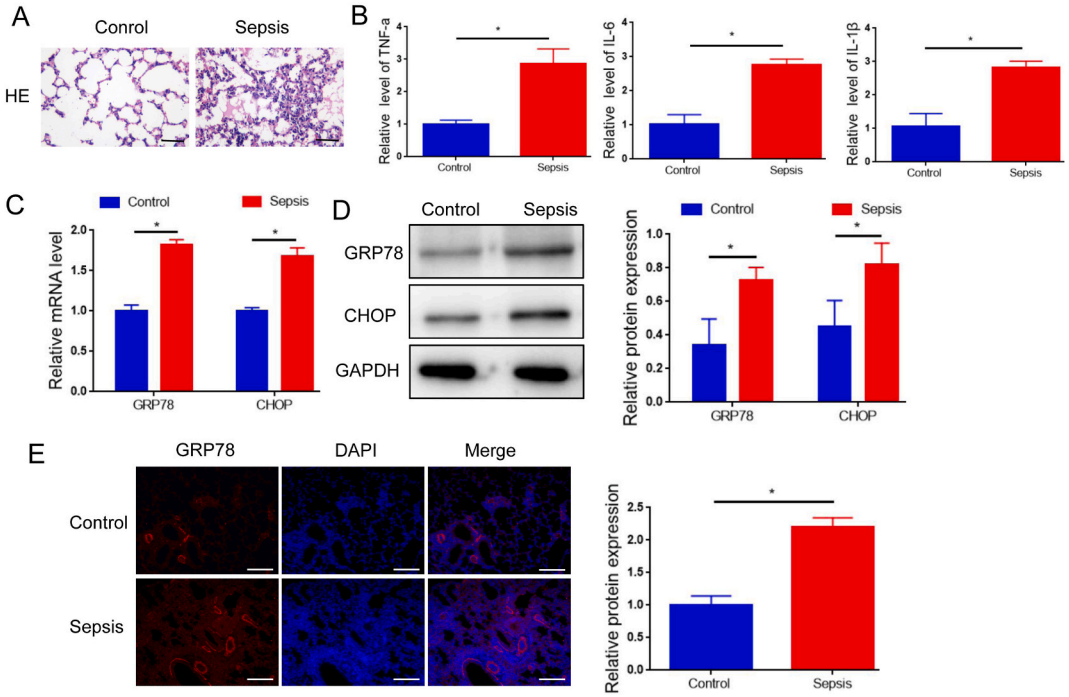

Fig. 1. Characterization of the septic mouse model. HE staining of lung tissues from septic mice and the control mice. B. qRT-PCR analysis of serum levels of TNF-a, IL-6, IL-1β in the septic mice and the control mice. C. qRT-PCR analysis of the mRNA levels of GRP78 and CHOP in the lung tissues of the septic mice and the control mice. D. Western blot analysis of the protein levels of GRP78 and CHOP in the lung tissues of the septic mice and the control mice. E. Immunofluorescence staining detecting the protein levels of GRP78 and CHOP in the lung tissues of the septic mice and the control mice. Scale bar = 50 μm. Data was presented as means ± SD from three independent experiments. Statistical analysis was performed using Student's t-test. **P < 0.01.

2.15. HE staining

Lung tissues embedded in paraffin were cut to 4 μm-thick sections. Sections were deparaffinized and rehydrated with distilled water. Sections were stained with hematoxylin (5 min) and eosin (2 min). Images were captured using a light microscope.

2.16. Statistical analysis

All data were represented as the mean ± standard deviation (SD). Statistical analysis was performed using the SPSS statistical software (SPSS, Chicago). Student's T-test was used for comparison between two groups, while One-way ANOVA with Tukey post-test was used for multiple comparisons. Statistical significance was defined as $P < 0.05$.

3. Results

3.1. Characterization of the septic mouse model

The septic mouse model was developed through CLP surgery. HE staining revealed a significant increase in lung tissue damage in septic mice compared to control mice (Fig. 1A), which is consistent with the findings in a previous study [27]. qRT-PCR assay demonstrated noticeably higher levels of inflammatory chemokines (TNF-a, IL-6, IL-1β) in the serum of septic mice compared to control mice (Fig. 1B). These findings confirmed the successful establishment of the CLP model. Additionally, mRNA levels of two markers of endoplasmic reticulum (ER) stress activation, glucose-regulated protein 78 (GRP78) and C/EBP homologous protein (CHOP) [28] were significantly higher in septic mice compared to control mice (Fig. 1C). Consistently, Western blotting and immunofluorescence staining revealed remarkable elevation of GRP78 and CHOP protein levels in the lung tissues of septic mice compared to control mice (Fig. 1D and E). To further confirm ER stress in septic mice, analysis of ER morphology in lung tissues was conducted using transmission electron microscopy. Results showed a normal ER structure in the lung tissues of control mice, while dilated ER cisternae were observed in the lung tissues of septic mice (Fig. S1).

3.2. Isolation and identification of BMSC-derived exosomes

To investigate the therapeutic efficacy of BMSC-derived exosomes on lung injury induced by sepsis, we isolated exosomes from BMSCs cultured in medium with (IB-exos) or without (B-exos). The morphology of the isolated exosomes was examined using transmission electron microscopy and exhibited a spherical shape (Fig. 2A). The size distribution of the exosomes was determined by NTA and showed diameters ranging from 50 to 150 nm (Fig. 2B). Western blot analysis revealed comparable expression levels of exosome markers (CD9, CD81, and TSG-101) in both B-exos and IB-exos (Fig. 1C). Additionally, we assessed the uptake of the exosomes by HUVECs using an immunofluorescence staining assay. The results indicate that both PKH67-labeled B-exos and IB-exos are successfully internalized by HUVECs (Fig. 1D).

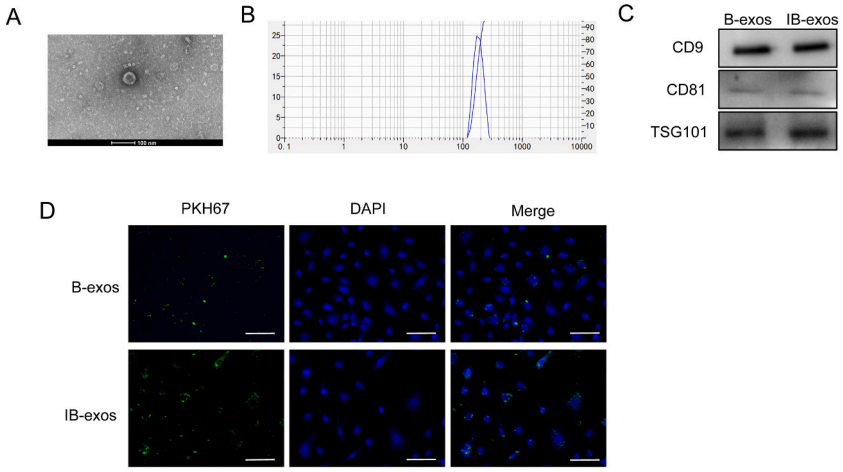

Fig. 2. Characterization of exosomes isolated from MSCs pretreated with or without IL-1β. A. The exosome morphology was analyzed by transmission electron microscopy. B. The diameter of exosomes was detected by NTA analysis. C. The expression of CD9, CD81, and TSG101 in B-exos or IB-exos was analyzed by Western blot analysis. D. The uptake of B-exos or IB-exos by HUVECs was detected by immunofluorescence staining. Scale bar = 50 μm.

3.3. IB-exos suppress LPS-induced sepsis in HUVECs

In light of the critical role of endothelial cell injury in the development of sepsis-induced lung injury [29], an in vitro LPS-induced sepsis cell model was established by treating HUVECs with LPS. qRT-PCR analysis revealed a significant upregulation of TNF-α, IL-6, and IL-1β mRNA levels in the HUVECs after LPS administration (Fig. 3A), thereby confirming the successful establishment of the sepsis cell model. The effects of IB-exos on HUVEC viability were examined using an EDU proliferation assay, which demonstrated that IB-exos improved cell viability that was reduced by LPS, and the efficacy of IB-exos was superior to that of B-exos (Fig. 3B). The apoptotic rate of HUVECs was also decreased more effectively by IB-exos than by B-exos (Fig. 3C). Furthermore, a Transwell migration assay revealed that exosomes rescued the motility of HUVECs that had been impaired by LPS, and the impact of IB-exos on migration was stronger than that of B-exos (Fig. 3D). Additionally, IB-exos caused a more substantial increase in the tube formation ability of HUVECs compared with B-exos, as confirmed by the tube formation assay (Fig. 3E).

Next, we investigated the impact of exosomes on ER stress response by examining the expression of GRP78 and CHOP. Our qRT-PCR analysis revealed that LPS treatment led to increased levels of GRP78 and CHOP mRNA in HUVECs. However, when exosomes were administered, these effects were reversed. Notably, the reduction in GRP78 and CHOP expression was more pronounced in HUVECs treated with IB-exos compared to those treated with B-exos (Fig. 4A–B). Similarly, the protein levels of GRP78 and CHOP were lower in the IB-exos group compared to the B-exos group (Fig. 4C and D, and Fig. S2). Taken together, these results indicate that pretreatment with IL-1β enhances the therapeutic potential of exosomes in the treatment of LPS-induced sepsis by inhibiting ER stress.

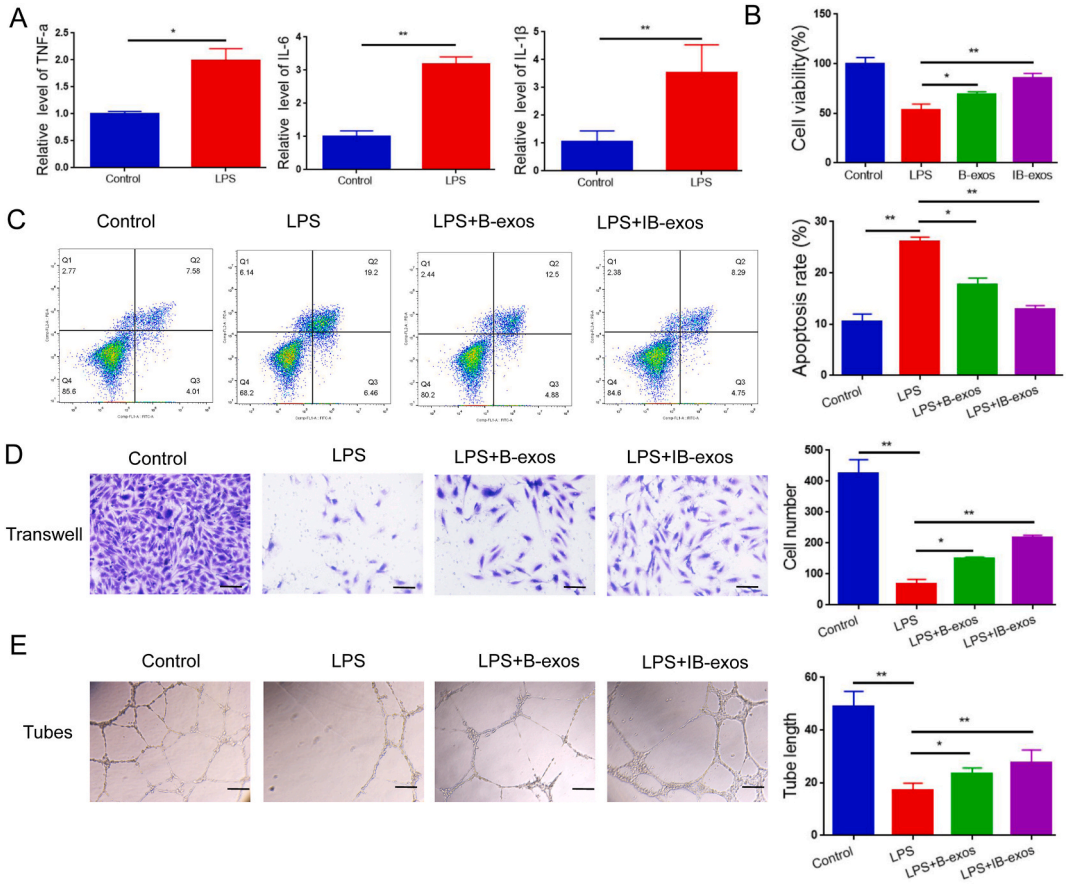

Fig. 3. IB-exos enhance cellular function of LPS-treated HUVECs. A. The content of TNF-a, IL-6, and IL-1β in HUVECs treated with or without LPS was determined by ELISA assay. B. The cell viability of HUVECs with different treatments (Control, LPS, LPS + B-exos, LPS + IB-exos) was determined by EDU proliferation assay. C. The apoptosis of HUVECs with different treatments (Control, LPS, LPS + B-exos, LPS + IB-exos) was determined by flow cytometry assay. D. The motility of HUVECs with different treatments (Control, LPS, LPS + B-exos, LPS + IB-exos) was determined by migration assay. E. The tube formation ability of HUVECs with different treatments (Control, LPS, LPS + B-exos, LPS + IB-exos) was determined by tube formation assay. Scale bar = 50 μm. Data was presented as means ± SD from three independent experiments. Statistical analysis was performed using one-way ANOVA. *P < 0.05, **P < 0.01.

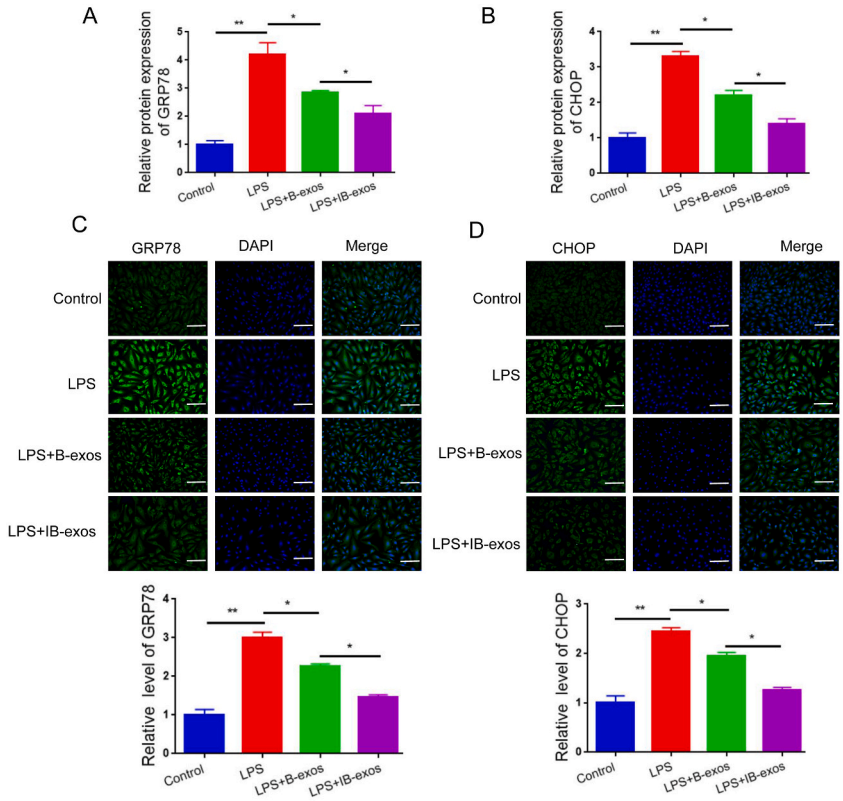

Fig. 4. IB-exos inhibit ER stress in HUVECs. A-B. The mRNA levels of GRP78 and CHOP were detected by qRT-PCR in HUVECs with different treatments (Control, LPS, LPS + B-exos, LPS + IB-exos). *C*-D. The protein levels of GRP78 and CHOP were detected by immunofluorescence staining in HUVECs with different treatments (Control, LPS, LPS + B-exos, LPS + IB-exos). Scale bar = 50 μm. Data was presented as means ± SD from three independent experiments. Statistical analysis was performed using one-way ANOVA. *P < 0.05, **P < 0.01.

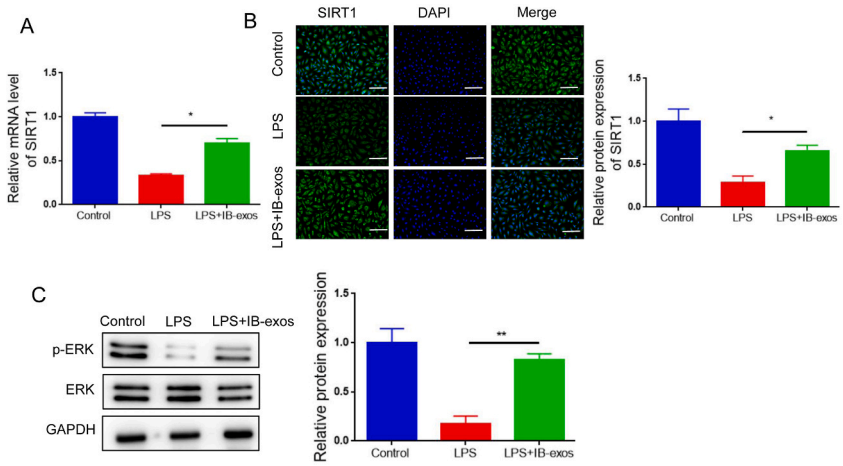

Fig. 5. IB-exos restore SIRT1 expression and ERK phosphorylation that are reduced by LPS in HUVECs. A. The mRNA level of SIRT1 was examined by qRT-PCR in HUVECs with different treatments (Control, LPS, LPS + IB-exos). B. The protein level of SIRT1 was examined by immunofluorescence staining in HUVECs with different treatments (Control, LPS, LPS + IB-exos). Scale bar = 50 μm. C. The levels of ERK and *p*-ERK were examined by Western blotting in HUVECs with different treatments (Control, LPS, LPS + IB-exos). Data was presented as means ± SD from three independent experiments. Statistical analysis was performed using one-way ANOVA. *P < 0.05, **P < 0.01.

3.4. IB-exos suppress LPS-induced sepsis via the SIRT1/ERK pathway

Sirtuin 1 (SIRT1) is a post-translational regulatory protein that plays a crucial role in ER stress. Hence, we investigated that whether IB-exos could modulate ER stress associated with sepsis by influencing SIRT1. We utilized qRT-PCR to analyze mRNA levels of SIRT1. The results demonstrated that LPS treatment reduced the mRNA expression of SIRT1, whereas treatment with IB-exos restored its mRNA level (Fig. 5A). Similarly, Western blot analysis revealed that LPS suppressed the protein level of SIRT1, but IB-exo treatment increased its level (Fig. 5B). Additionally, we assessed whether IB-exos could affect the phosphorylation status of ERK, a downstream effector of SIRT1. Western blot analysis demonstrated that LPS reduced the phosphorylation level of ERK, but treatment with IB-exos reversed this effect (Fig. 5C).

Next, we investigated whether SIRT1 is required for the function of IB-exos in LPS-induced sepsis. Our analysis of cell viability indicated that the treatment with IB-exos leads to an increase in HUVEC growth, while silencing SIRT1 reverses this effect (Fig. 6A). Furthermore, the migration assay revealed that IB-exos enhance the migratory ability of HUVECs, but knockdown of SIRT1 results in a reduction in the migration of the cells (Fig. 6B). Flow cytometry analysis also demonstrated that depleting SIRT1 increased the apoptotic rate that was decreased by IB-exos (Fig. 6C). Additionally, IB-exos decreased the expression levels of GRP78 and CHOP in HUVECs, whereas knockdown of SIRT1 resulted in an increase in the protein levels of these two markers (Fig. 7A). Our data also showed that silencing of SIRT1 resulted in a reversal of the inhibitory effect of IB-exos on ERK phosphorylation (Fig. 7B). Taken together, these results indicate that IB-exos can effectively suppress ER stress through activating the SIRT1/ERK signaling pathway.

3.5. IB-exos alleviate sepsis-induced lung injury in mice

Next, we addressed the therapeutic capability of IB-exos in vivo using a mouse model of sepsis induced by CLP. Histological analysis revealed that the administration of exosomes alleviated the lung damage in septic mice, with less damage observed in the IB-exos

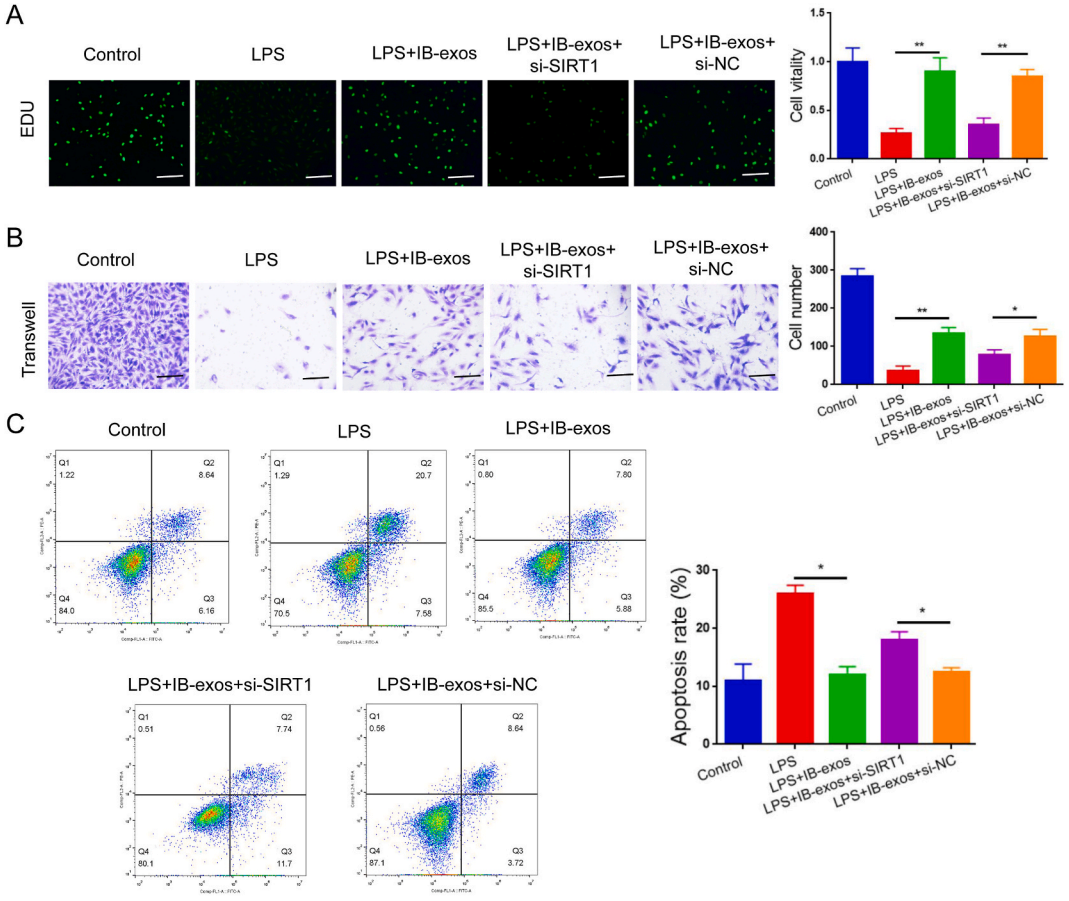

Fig. 6. Silencing of SIRT1 blocks the effects of IB-exos on the biological functions of HUVECs. A. EDU proliferation assay showing that silencing of SIRT1 decreased the viability of LPS-treated HUVECs that was enhanced by IB-exos. Scale bar = 50 μm. B. Transwell migration assay showing that silencing of SIRT1 decreased the motility of LPS-treated HUVECs that was elevated by IB-exos. C. Flow cytometry assay showing that silencing of SIRT1 increased the apoptosis of LPS-treated HUVECs that was reduced by IB-exos. Data was presented as means ± SD from three independent experiments. Statistical analysis was performed using one-way ANOVA. *P < 0.05, **P < 0.01.

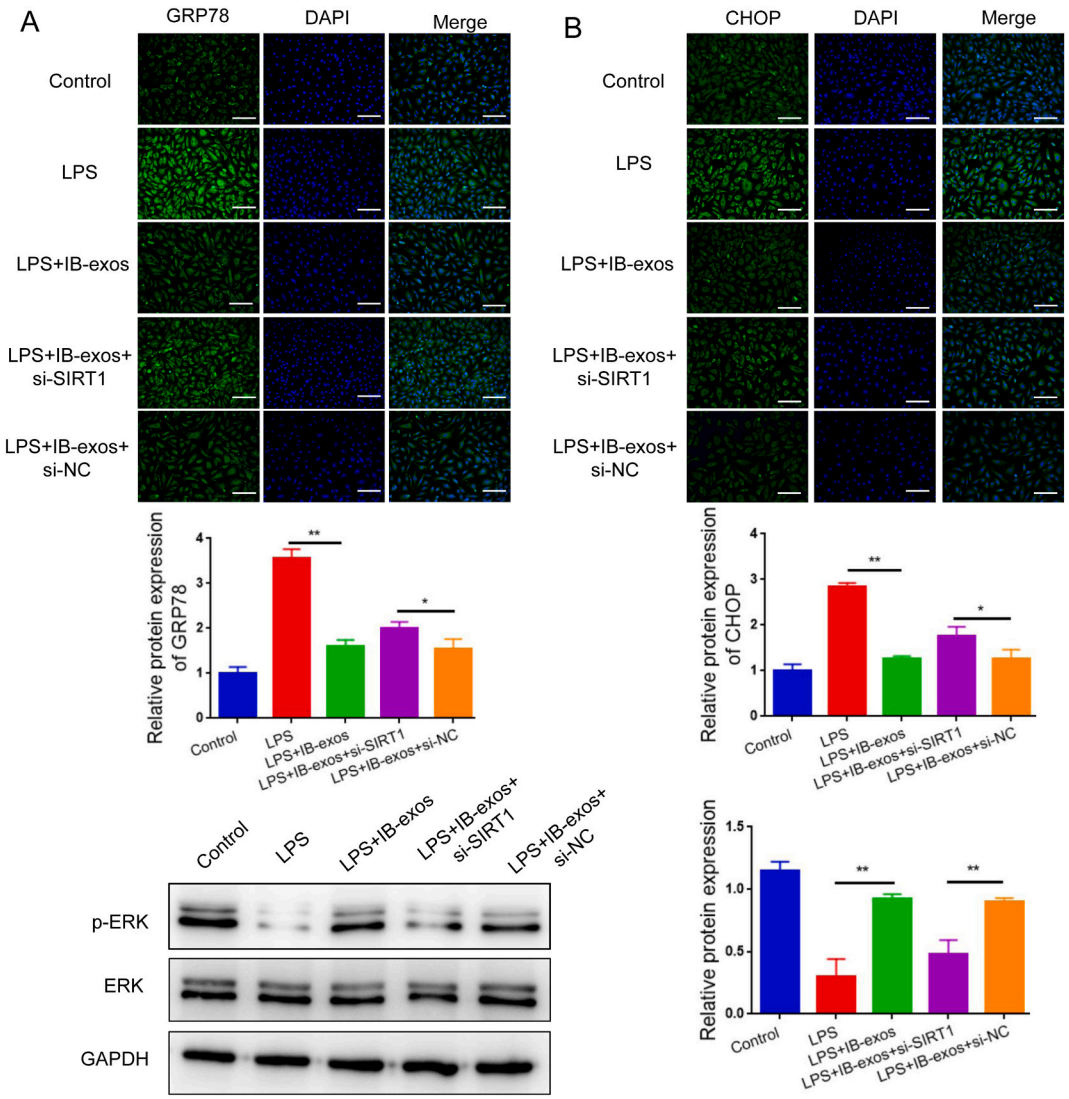

Fig. 7. Knockdown of SIRT1 reverses the effect of IB-exos on ER stress response. A. Immunofluorescence staining showing that knockdown of SIRT1 increased the expression levels of GRP78 and CHOP that were inhibited by IB-exos in LPS-treated HUVECs. Scale bar = 50 μm. B. Western blotting showing that knockdown of SIRT1 enhanced the phosphorylation of ERK that was reduced by IB-exos in LPS-treated HUVECs. Data was presented as means ± SD from three independent experiments. Statistical analysis was performed using one-way ANOVA. *P < 0.05, **P < 0.01.

group compared to the B-exos group (Fig. 8A). Treatment with exosomes led to a decrease in the serum levels of pro-inflammatory factors, such as TNF-a, and IL-6, and IL-1β. The reduction in these factors was more pronounced in the IB-exos group compared to the B-exos group (Fig. 8B). Additionally, the expression of SIRT1 was higher in the lung tissues of the IB-exos group compared to the B-exos group (Fig. 8C). Moreover, the mRNA and protein levels of GRP78 and CHOP were reduced after exosome administration, and this reduction was more significant in the IB-exos group compared to the B-exos group (Fig. 8C–D). Collectively, these results indicate that IB-exos exhibit protective effects against sepsis-induced lung injury by inhibiting ER stress through the upregulation of SIRT1.

4. Discussion

Sepsis is a severe and life-threatening disorder with high mortality rates, necessitating the development of new strategies. In this study, we discovered that pretreatment with IL-1β improved the therapeutic effects of exosomes derived from MSCs in both in vitro LPS-induced sepsis and in vivo CLP-induced sepsis. Our findings demonstrate that IB-exos activate the SIRT1/ERK signaling pathway, leading to the inhibition of ER stress response, and ultimately alleviating sepsis-induced lung injury.

ER stress is a response to the accumulation of misfolded or unfolded proteins and is known to contribute to the development of sepsis. For example, studies have shown that CLP treatment increases ER stress in lymphocytes, leading to lymphocyte apoptosis during sepsis [30]. Additionally, CLP triggers TIMP2-mediated ER stress, resulting in acute kidney injury in septic mice [9]. In rats, CLP

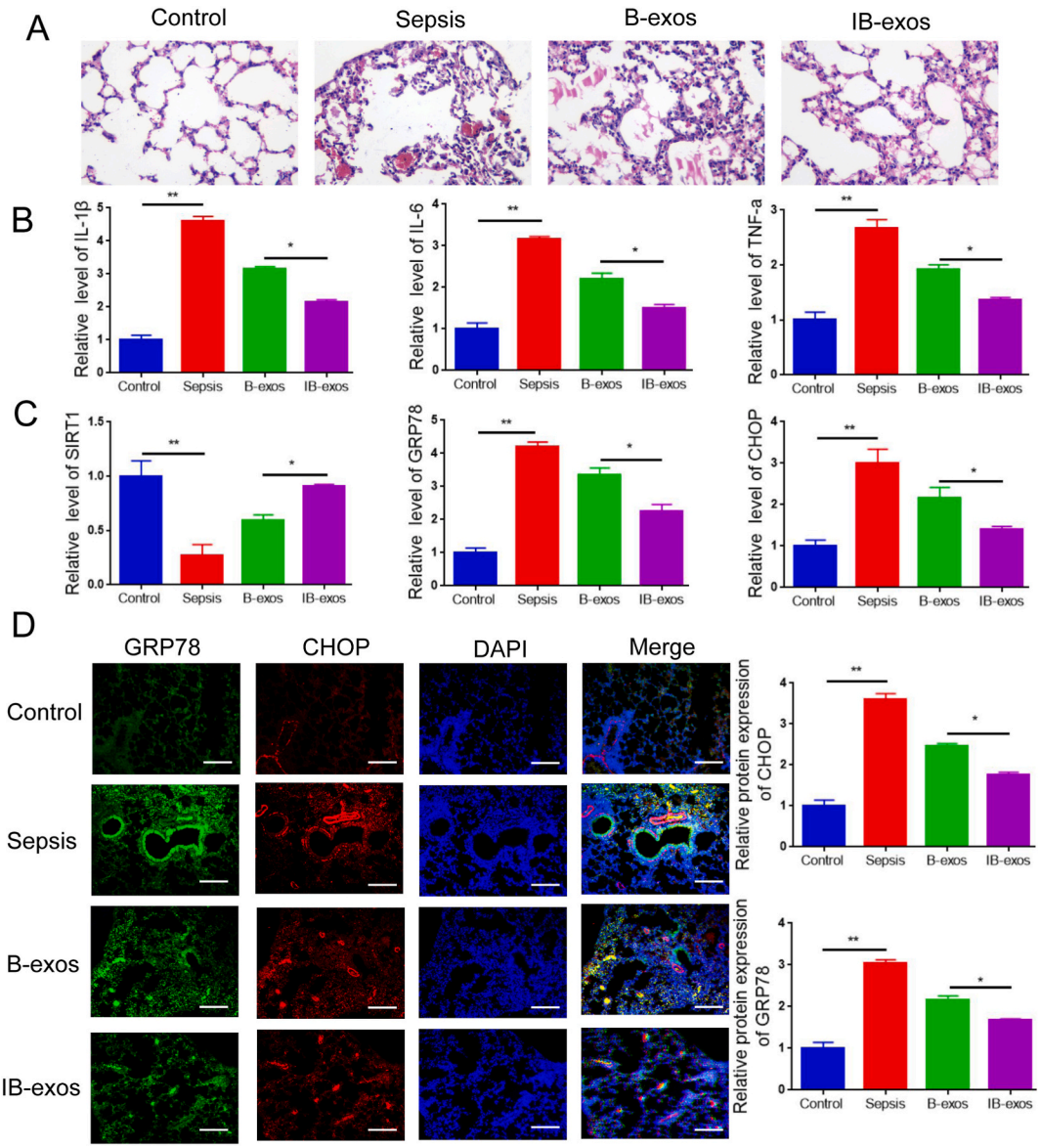

Fig. 8. IB-exos mitigate sepsis-induced lung injury in mice. A. The histology of the lung tissues in different groups (Control, Sepsis, B-exos, IB-exos) were accessed by HE staining (n = 6). B. The serum content of TNF-a, IL-6, IL-1β in different groups of mice (Control, Sepsis, B-exos, IB-exos) were accessed by ELISA (n = 6). C. The mRNA levels of SIRT1, GRP78, and CHOP in the lung tissues of different groups of mice (Control, Sepsis, B-exos, IB-exos) were accessed by qRT-PCR (n = 6). D. The protein levels of GRP78, and CHOP in the lung tissues of different groups of mice (Control, Sepsis, B-exos, IB-exos) were accessed by immunofluorescence staining (n = 6). Scale bar = 50 μm. Statistical analysis was performed using one-way ANOVA. *P < 0.05, **P < 0.01.

operation activates ER stress-mediated apoptosis, which in turn caused liver damage in sepsis [28]. Consistent with these studies, our data demonstrated that the expression of GRP78 and CHOP, which are recognized markers of ER stress activation, was significantly increased in HUVECs treated with LPS and in septic mice. This confirms the involvement of ER stress in sepsis. Administration of MSCs-exos has been identified as a promising strategy for treating various diseases, including sepsis. MSC-exos exert their therapeutic effect against sepsis by suppressing inflammation, apoptosis, and ER stress [20]. Our data further supported this notion by showing that treatment with IB-exos in an in vitro sepsis cell model increased cell viability, motility, and tube formation, while decreased apoptosis and ER stress in HUVECs. Moreover, in a CLP-induced mouse model, treatment with IB-exos reduced inflammation and ER stress response, and alleviated sepsis-induced lung injury.

SIRT1, a class-III histone deacetylase [31], plays a crucial role in various biological processes, including maintenance of genome stability, cell growth, survival, apoptosis, inflammation, and aging [32,33]. SIRT1 has been considered as a potential therapeutic target for diseases such as autoimmune diseases, diabetes, ischemia, Alzheimer's disease, and cancer [31–35]. Several studies have also

highlighted the significance of SIRT1 in sepsis progression. For instance, research suggests that SIRT1 contributes to the improvement of sepsis-induced acute kidney injury by inducing deacetylation-mediated autophagy through Beclin1 [36]. Furthermore, SIRT1 has been found to alleviate sepsis-mediated lung injury by inhibiting endoplasmic reticulum stress and inflammation [37].

Consistent with previous studies, our results demonstrated that administration of LPS decreased the expression of SIRT1 in HUVECs. However, treatment with IB-exos restored the abundance of SIRT1. Furthermore, when SIRT1 was knocked down, the inhibitory effect of IB-exos on ER stress was blocked, and the promoting effects of IB-exos on HUVEC proliferation and migration were counteracted. In vivo experiments confirmed that IB-exos increased the expression of SIRT1 and suppressed the ER stress response, leading to alleviated lung injury in septic mice. It has been reported that ERK is a downstream factor of SIRT1, and ERK signaling is involved in the modulation of ER stress [38–40]. Consistently, treatment with IB-exos elevated the expression of SIRT1, accompanied by increased phosphorylation of ERK. Collectively, our findings suggest that IB-exos mitigate septic ER stress response by activating the SIRT1/ERK cascade.

5. Conclusions

In this study, we have identified that IB-exos have the ability to mitigate sepsis-induced lung injury. The beneficial effects of IB-exos are achieved through the suppression of ER stress, which is accomplished by activating the SIRT1/ERK pathway. These findings indicate that IB-exos could potentially be utilized as a novel treatment strategy for sepsis.

Ethics statement

The study was approved by the Institutional Animal Care and Use Committee of Union Shenzhen Hospital of Huazhong University of Science and Technology (SYT23006).

Consent for publication

All authors Consent for publication.

Author contribution statement

Conceived and designed the experiments: Weiwei Ding, Xinsheng Cheng.Performed the experiments: Shikai Wang, Zhipeng Li. Analyzed and interpreted the data: Jianguo Wu, Di He. Contributed reagents, materials, analysis tools or data: Xinsheng Cheng, Shikai Wang.Wrote the paper: Weiwei Ding.

Funding statement

This work was supported by the Shenzhen Basic Research Project {JCYJ20190809101413443}, Shenzhen Nanshan District science and technology plan key project {2020005}, Hospital project of Union Shenzhen Hospital of Huazhong University of Science and Technology {YN2020015}.

Data availability statement

Data will be made available on request.

Declaration of competing interest

The authors declare that they have no known competing financial interests or personal relationships that could have appeared to influence the work reported in this paper.

Abbreviations

CHOP	C/EBP homologous protein
CLP	Cecal ligation and puncture
DAMP	damage-associated molecular pattern
GRP78	Glucose-regulated protein 78
MSCs	Mesenchymal stem cells
ER	Endoplasmic reticulum

Appendix A. Supplementary data

Supplementary data to this article can be found online at https://doi.org/10.1016/j.heliyon.2023.e20124.

References

[1] A. Purcarea, S. Sovaila, Sepsis, a 2020 review for the internist, Rom. J. Intern. Med. 58 (2020) 129–137.
[2] T. Gong, Y. Liu, Z. Tian, M. Zhang, H. Gao, Z. Peng, S. Yin, C.W. Cheung, Y. Liu, Identification of immune-related endoplasmic reticulum stress genes in sepsis using bioinformatics and machine learning, Front. Immunol. 13 (2022), 995974.
[3] T. van der Poll, F.L. van de Veerdonk, B.P. Scicluna, M.G. Netea, The immunopathology of sepsis and potential therapeutic targets, Nat. Rev. Immunol. 17 (2017) 407–420.
[4] R. Wen, Y.P. Liu, X.X. Tong, T.N. Zhang, N. Yang, Molecular mechanisms and functions of pyroptosis in sepsis and sepsis-associated organ dysfunction, Front. Cell. Infect. Microbiol. 12 (2022), 962139.
[5] A. Sang, Y. Wang, S. Wang, Q. Wang, X. Wang, X. Li, X. Song, Quercetin attenuates sepsis-induced acute lung injury via suppressing oxidative stress-mediated ER stress through activation of SIRT1/AMPK pathways, Cell. Signal. 96 (2022), 110363.
[6] L.A. Perera, D. Ron, AMPylation and endoplasmic reticulum protein folding homeostasis, Cold Spring Harbor Perspect. Biol. 15 (2023).
[7] Y. Xia, J. Zhu, R. Yang, H. Wang, Y. Li, C. Fu, Mesenchymal stem cells in the treatment of spinal cord injury: mechanisms, current advances and future challenges, Front. Immunol. 14 (2023), 1141601.
[8] H. Tran, A. Mittal, V. Sagi, K. Luk, A. Nguyen, M. Gupta, J. Nguyen, Y. Lamarre, J. Lei, A. Guedes, K. Gupta, Mast cells induce blood brain barrier damage in SCD by causing endoplasmic reticulum stress in the endothelium, Front. Cell. Neurosci. 13 (2019) 56.
[9] N. Jiang, R. Huang, J. Zhang, D. Xu, T. Li, Z. Sun, L. Su, Z. Peng, TIMP2 mediates endoplasmic reticulum stress contributing to sepsis-induced acute kidney injury, Faseb. J. 36 (2022), e22228.
[10] D.C. Ding, W.C. Shyu, S.Z. Lin, Mesenchymal stem cells, Cell Transplant. 20 (2011) 5–14.
[11] J. Liu, Y. Zhou, C. Xie, C. Li, L. Ma, Y. Zhang, Anti-ferroptotic effects of bone marrow mesenchymal stem cell-derived extracellular vesicles loaded with ferrostatin-1 in cerebral ischemia-reperfusion injury associate with the GPX4/COX-2 Axis, Neurochem. Res. 48 (2023) 502–518.
[12] T.J. Wannemuehler, M.C. Manukyan, B.D. Brewster, J. Rouch, J.A. Poynter, Y. Wang, D.R. Meldrum, Advances in mesenchymal stem cell research in sepsis, J. Surg. Res. 173 (2012) 113–126.
[13] E. El Agha, R. Kramann, R.K. Schneider, X. Li, W. Seeger, B.D. Humphreys, S. Bellusci, Mesenchymal stem cells in fibrotic disease, Cell Stem Cell 21 (2017) 166–177.
[14] V.K. Mishra, H.H. Shih, F. Parveen, D. Lenzen, E. Ito, T.F. Chan, L.Y. Ke, Identifying the therapeutic significance of mesenchymal stem cells, Cells (2020) 9.
[15] A. Khosrojerdi, S. Soudi, A.Z. Hosseini, F. Eshghi, A. Shafiee, S.M. Hashemi, Immunomodulatory and therapeutic effects of mesenchymal stem cells on organ dysfunction in sepsis, Shock 55 (2021) 423–440.
[16] L. Ge, J. Zhao, H. Deng, C. Chen, Z. Hu, L. Zeng, Effect of bone marrow mesenchymal stromal cell therapies in rodent models of sepsis: a meta-analysis, Front. Immunol. 12 (2021), 792098.
[17] E. Alp, Z.B. Gonen, K. Gundogan, A. Esmaoglu, L. Kaynar, A. Cetin, M. Karakukcu, M. Cetin, G. Kalin, M. Doganay, The effect of mesenchymal stromal cells on the mortality of patients with sepsis and septic shock: a promising therapy, Emerg Med Int 2022 (2022), 9222379.
[18] Q. Cao, C. Huang, X.M. Chen, C.A. Pollock, Mesenchymal stem cell-derived exosomes: toward cell-free therapeutic strategies in chronic kidney disease, Front. Med. 9 (2022), 816656.
[19] O. Cho, D.W. Kim, J.Y. Cheong, Screening plasma exosomal RNAs as diagnostic markers for cervical cancer: an analysis of patients who underwent primary chemoradiotherapy, Biomolecules 11 (2021).
[20] M.D. Chiang, C.Y. Chang, H.J. Shih, V.L. Le, Y.H. Huang, C.J. Huang, Exosomes from human placenta choriodecidual membrane-derived mesenchymal stem cells mitigate endoplasmic reticulum stress, inflammation, and lung injury in lipopolysaccharide-treated obese mice, Antioxidants (2022) 11.
[21] L. Zhao, L. Yu, X. Wang, J. He, X. Zhu, R. Zhang, A. Yang, Mechanisms of function and clinical potential of exosomes in esophageal squamous cell carcinoma, Cancer Lett. 553 (2023), 215993.
[22] A. Murao, M. Brenner, M. Aziz, P. Wang, Exosomes in sepsis, Front. Immunol. 11 (2020) 2140.
[23] R. Zhang, Y. Zhu, Y. Li, W. Liu, L. Yin, S. Yin, C. Ji, Y. Hu, Q. Wang, X. Zhou, J. Chen, W. Xu, H. Qian, Human umbilical cord mesenchymal stem cell exosomes alleviate sepsis-associated acute kidney injury via regulating microRNA-146b expression, Biotechnol. Lett. 42 (2020) 669–679.
[24] Y. Shi, Y. Wang, Q. Li, K. Liu, J. Hou, C. Shao, Y. Wang, Immunoregulatory mechanisms of mesenchymal stem and stromal cells in inflammatory diseases, Nat. Rev. Nephrol. 14 (2018) 493–507.
[25] H. Liu, X. Zhu, X. Cao, A. Chi, J. Dai, Z. Wang, C. Deng, M. Zhang, IL-1beta-primed mesenchymal stromal cells exert enhanced therapeutic effects to alleviate Chronic Prostatitis/Chronic Pelvic Pain Syndrome through systemic immunity, Stem Cell Res. Ther. 12 (2021) 514.
[26] B. Wei, Y. Ma, Synergistic effect of GF9 and streptomycin on relieving gram-negative bacteria-induced sepsis, Front. Bioeng. Biotechnol. 10 (2022), 973588.
[27] Z. Cao, H. Qin, Y. Huang, Y. Zhao, Z. Chen, J. Hu, Q. Gao, Crosstalk of pyroptosis, ferroptosis, and mitochondrial aldehyde dehydrogenase 2-related mechanisms in sepsis-induced lung injury in a mouse model, Bioengineered 13 (2022) 4810–4820.
[28] W.J. Qian, Q.H. Cheng, Endoplasmic reticulum stress-mediated apoptosis signal pathway is involved in sepsis-induced liver injury, Int. J. Clin. Exp. Pathol. 10 (2017) 9990–9997.
[29] M. Gao, T. Yu, D. Liu, Y. Shi, P. Yang, J. Zhang, J. Wang, Y. Liu, X. Zhang, Sepsis plasma-derived exosomal miR-1-3p induces endothelial cell dysfunction by targeting SERP1, Clin. Sci. (Lond.) 135 (2021) 347–365.
[30] T. Ma, L. Han, Y. Gao, L. Li, X. Shang, W. Hu, C. Xue, The endoplasmic reticulum stress-mediated apoptosis signal pathway is involved in sepsis-induced abnormal lymphocyte apoptosis, Eur. Surg. Res. 41 (2008) 219–225.
[31] X. Meng, J. Tan, M. Li, S. Song, Y. Miao, Q. Zhang, Sirt1: role under the condition of ischemia/hypoxia, Cell. Mol. Neurobiol. 37 (2017) 17–28.
[32] D.K. Alves-Fernandes, M.G. Jasiulionis, The role of SIRT1 on DNA damage response and epigenetic alterations in cancer, Int. J. Mol. Sci. 20 (2019).
[33] Y. Yang, Y. Liu, Y. Wang, Y. Chao, J. Zhang, Y. Jia, J. Tie, D. Hu, Regulation of SIRT1 and its roles in inflammation, Front. Immunol. 13 (2022), 831168.
[34] F. Jiao, Z. Gong, The beneficial roles of SIRT1 in neuroinflammation-related diseases, Oxid. Med. Cell. Longev. 2020 (2020), 6782872.
[35] M.P. Jalgaonkar, U.M. Parmar, Y.A. Kulkarni, M.J. Oza, SIRT1-FOXOs activity regulates diabetic complications, Pharmacol. Res. 175 (2022), 106014.
[36] Z. Deng, M. Sun, J. Wu, H. Fang, S. Cai, S. An, Q. Huang, Z. Chen, C. Wu, Z. Zhou, H. Hu, Z. Zeng, SIRT1 attenuates sepsis-induced acute kidney injury via Beclin1 deacetylation-mediated autophagy activation, Cell Death Dis. 12 (2021) 217.
[37] F. Wang, J. Ma, J. Wang, M. Chen, H. Xia, S. Yao, D. Zhang, SIRT1 ameliorated septic associated-lung injury and macrophages apoptosis via inhibiting endoplasmic reticulum stress, Cell. Signal. 97 (2022), 110398.
[38] J. Huang, Q. Gan, L. Han, J. Li, H. Zhang, Y. Sun, Z. Zhang, T. Tong, SIRT1 overexpression antagonizes cellular senescence with activated ERK/S6k1 signaling in human diploid fibroblasts, PLoS One 3 (2008), e1710.
[39] J. Zhang, L. Wang, W. Xie, S. Hu, H. Zhou, P. Zhu, H. Zhu, Melatonin attenuates ER stress and mitochondrial damage in septic cardiomyopathy: a new mechanism involving BAP31 upregulation and MAPK-ERK pathway, J. Cell. Physiol. 235 (2020) 2847–2856.
[40] H. Zou, G. Liu, Inhibition of endoplasmic reticulum stress through activation of MAPK/ERK signaling pathway attenuates hypoxia-mediated cardiomyocyte damage, J. Recept. Signal Transduct. Res. 41 (2021) 532–537.